Journal of Materials Chemistry

Dynamic Article Links

Cite this: J. Mater. Chem., 2012, 22, 20929

www.rsc.org/materials

PAPER

# Investigation of Hg sorption and diffusion behavior on ultra-thin films of gold using QCM response analysis and SIMS depth profiling†

**Ylias M. Sabri,*[a] Samuel J. Ippolito,[a] Mohammad Al Kobaisi,[b] Matthew J. Griffin,[a] David R. Nelson[c] and Suresh K. Bhargava*[a]**

***Received 22nd June 2012, Accepted 30th July 2012***
**DOI: 10.1039/c2jm34053d**

Using the quartz crystal microbalance (QCM) technique, we demonstrate that the contribution of Hg adsorption and absorption on the sensor response profile can be distinguished by studying the dynamic response curve of QCM based Hg vapor sensors that employ an ultra-thin film of Au in the range of 10 to 40 nm thickness as the sensitive layer. The response magnitudes of the QCMs were extrapolated to zero thickness (ETZT) in an attempt to determine the contribution of adsorbed Hg on the sensor response magnitude and response profile. In general, the ratio of adsorbed to absorbed Hg on Au films is found to decrease with increased Hg vapor concentration. Furthermore, the same ratio was observed to decrease with increasing Au film thickness. The 10 nm and 40 nm Au films for example were found to contain adsorbed Hg content of 43.8% and 16.4%, respectively, with the balance attributed to absorption/amalgamation, when exposed to Hg vapor concentration of 10.55 mg $m^{-3}$ for a period of 14 hours and an operating temperature of 28 °C. In addition, the QCMs were characterized using secondary ion mass spectroscopy depth profiling in order to study the diffusion behaviour of Hg in the Au surfaces. It is deduced that in order to reduce Hg accumulation in Au thin films, a non-continuous type film (similar to the 10 nm ultra-thin Au sensitive layer morphology) would be more functional as a Hg sensitive layer where quick absorption and desorption processes are required.

## Introduction

Mercury (Hg) emitted from industrial sources is now recognized as a major concern by governments and environmental bodies worldwide due to the acute health and environmental risks associated with its release into the atmosphere.[1,2] The continuous monitoring followed by controlling and limiting the level of these emissions is an important factor in increasing the sustainability of many industrial processes worldwide. In this regard, a significant amount of work has recently focused on developing optical and solid-state Hg sensors as an alternative to what is available commercially.[3–6] Generally solid-state Hg sensors work on mercury amalgamation or chemi-sorption principles between Hg and a selective layer material which overlays a micro-machined transducer platform. Alternatively, optical based sensors function *via* reflectivity or absorption principles. Work spanning the last few decades has seen the use of Au thin-films as a sensitive material for mercury sensing applications which can be used in conjunction with reflective, resistive or mass based sensor platforms.[6–9] One such transducer platform is the quartz crystal microbalance (QCM), which is an example of a mass based transducer that has successfully been demonstrated as a potential mercury vapor sensor.[9] Recent work from our group has also shown Au based QCMs being highly selective towards mercury vapor in the presence of moisture and could potentially be used in environmental pollutant monitoring applications.[10] The QCM technique utilizes the linear relationship between the frequency shift ($\Delta f$) and the mass change ($\Delta m$) observed on the electrode surface given by:

$$\Delta f = -\frac{2f_0^2}{A\sqrt{c_{66}\rho_q}}\Delta m = -S_f\Delta m \quad (1)$$

here $S_f$ represents the integral mass sensitivity or Sauerbrey constant and is proportional to the square of the fundamental frequency, $f_0$, inversely proportional to the surface area, $A$, and

[a]*Advanced Materials and Industrial Chemistry (AMIC) Centre, School of Applied Sciences, RMIT University, Melbourne, Australia. E-mail: suresh.bhargava@rmit.edu.au; ylias.sabri@rmit.edu.au; Fax: +61 3 9925 3747; Tel: +61 3 9925 3365*

[b]*School of Applied Sciences, RMIT University, Melbourne, VIC 3001, Australia*

[c]*School of Natural Sciences, University of Western Sydney, Penrith South, NSW 1797, Australia*

† Electronic supplementary information (ESI) available: More detailed experimental details. Table S1: drift, noise and *Q*-factors of the QCMs with optically polished Au electrodes having thicknesses of either 40, 50, 100, 150 or 200 nm at operating temperatures of 28 and 89 °C. Fig. S1: SEM image of Au thin films before (left panel) and after (right panel) Hg exposure. Fig. S2: SIMS depth profile of Hg for all four ultra-thin Au sensitive layers exposed to a Hg concentration of 10.55 mg $m^{-3}$ at an operating temperature of 28 °C. See DOI: 10.1039/c2jm34053d

increases proportionally with the overtone number.[11] The parameters $c_{66}$ and $\rho_q$ are the shear modulus ($2.947 \times 10^{11}$ g cm$^{-1}$ s$^{-2}$) and density (2.648 g cm$^{-3}$) of the quartz substrate.

In order to use Au electrode transducers as mercury vapor sensors, the interaction process between Au and Hg needs to be better understood.[12] The lack of such understanding has prompted numerous studies in the literature trying to better understand the interaction of elemental Hg with Au thin films.[13–20] To further build on such understanding we have attempted to differentiate between Hg sorption processes on Au thin films by employing quartz crystal microbalance (QCM) transducers due to their high mass sensitivity (in ng cm$^{-2}$ Hz$^{-1}$ range) resulting in better resolution of mercury uptake kinetics data.

In addition to determining the proportion of adsorbed to that of absorbed/amalgamated Hg, the diffusion of Hg into ultra-thin Au sensitive layers by secondary ion mass spectroscopy (SIMS) depth profiling characterization is also presented in this study. Diffusion is the process of atoms in matter being randomly mobile from a point of higher concentration to lower concentration, and the mobility is proportional to this concentration gradient.[21] The Hg on Au with a relatively larger film thickness is therefore expected to migrate deeper within the bulk, where the Hg concentration gradient is lower relative to the upper surface of the film. The driving force of this is presumably so that the Hg distribution within the film reaches equilibrium. Furthermore, as the film thickness is increased during Au deposition, the kink and step defects propagate themselves throughout the growing phase[22] which also act as Hg sorption sites. In the case of using such films for Hg sensitive layers on QCM based sensors, it is well known that the sensitivity of a sensor towards elemental Hg vapor is dependent on Au film thickness.[23,24] The thicker the Au film the larger the QCM response magnitude expected due to a larger amount of Hg diffusion into the thicker film's depth.[25] The findings will provide insight into the type of Au surface modification techniques required to develop selective QCM based Hg vapor sensors.

## Experimental

The specially prepared multi-layered electrode QCMs were fabricated for this study. Each QCM was fabricated by evaporating 10 nm Ti and 150 nm Au thin films (4.5 mm diameter) to form the main electrodes of the QCM devices (7.5 mm diameter) using a Balzers™ electron beam evaporator with a specially designed shadow mask. Thereafter a 20 nm $SiO_2$ barrier layer followed by an ultra-thin Au sensitive layer with thicknesses of either 10, 20, 30 or 40 nm was deposited over the underlying Ti:10/Au:150 nm QCM electrodes. The 20 nm $SiO_2$ layer was employed as a barrier layer to stop any mercury from diffusing into the 150 nm Au film, which is used as the electrical contact of the QCM electrode as shown in Fig. 1.

A minimum thickness of 10 nm Au layer was chosen as it has been previously reported[26] that Au film thicknesses above 7.5 nm are required to form a continuous film. The 10 nm Au film chosen ensured the thinnest continuous film possible for the purpose of extrapolation to zero Au film thickness. The underlying 150 nm Au electrode was chosen due to its highest $Q$-factor

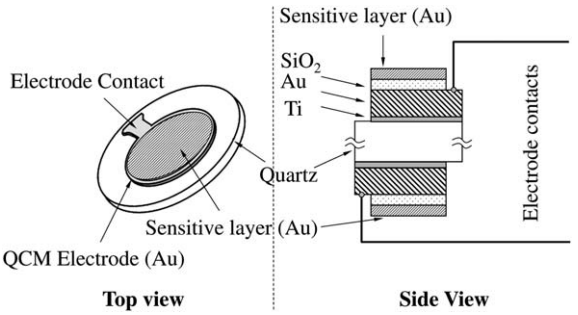


**Fig. 1** Ultra-thin Au sensitive layer based QCM. The outermost layer is comprised of the ultra thin films of Au (10–40 nm Au sensitive layer) and the inner Au layer is the QCM electrode having a thickness of 150 nm. The Ti adhesion layers and $SiO_2$ barrier layers are 10 and 20 nm in thickness, respectively.

compared to QCMs with other Au thicknesses (see Table S1 in the ESI†).

A set of 16 QCMs was prepared for each thickness of the ultra-thin Au sensitive layer. Selected QCMs were then exposed to Hg vapor concentrations of 1.02, 3.65 or 10.55 mg m$^{-3}$ at operating temperatures of 28, 55 or 89 °C (totalling 9 different operating conditions) at a constant gas flow of 200 sccm. The time of Hg exposure was 14 hours followed by 5 hours of recovery period under dry nitrogen atmosphere. It was determined, from preliminary experiments with extended desorption times, that the desorption of Hg beyond the initial 5 h time period is minimal, thus justifying the chosen 5 h desorption time used in the experiments.[27]

Following the controlled Hg vapor exposure, secondary ion mass spectroscopy (SIMS) (Cameca IMS 5f) depth profiles were performed using a $Cs^+$ primary ion beam of 3 keV net impact energy, a 1.5 nA beam current and a raster area of 500 μm × 500 μm. To eliminate potential edge effects, a combination of lens settings was used to restrict the secondary ion yield to a 100 μm diameter region within the centre of the rastered area. Surface topography was measured using an Alpha-step IQ Surface Profilometer (KLA Tencor Corporation). Due to the lack of availability of SIMS, the Au films of all 40 QCMs were characterised within a 3-day period, 4 weeks after being exposed to Hg vapor. SEM measurements were performed using a Nano-SEM instrument operating at an accelerating voltage of 10 kV.

## Results and discussions

### Extrapolation method (ETZT)

QCMs with different Au film thicknesses are expected to produce different signal output magnitudes ($\Delta f$ values) for each film thickness when exposed to identical Hg vapor concentration, operating temperature and Hg exposure period (see Fig. 2). The $\Delta f$ values obtained can then be extrapolated to zero Au film thickness with the result corresponding to Hg adsorption alone ($\Delta f_{ads}$). This method would enable the response magnitude contribution due to the adsorption component of the Hg–Au interaction process on an Au sensitive layer to be determined. The extrapolation to zero thickness (ETZT) is the key aspect of this method of separating such signals. It is based on assuming that the primary contributors to the QCM dynamic response are

 

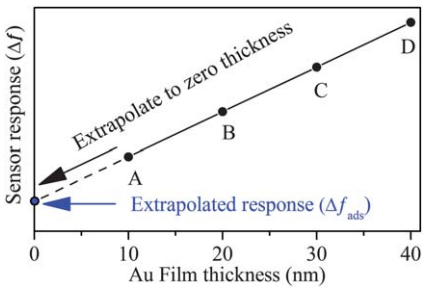


**Fig. 2** The extrapolation to zero thickness (ETZT) method by plotting the response magnitude of each QCM (having an ultra-thin Au sensitive layer with thicknesses of either 10, 20, 30 or 40 nm) following their exposure to Hg vapor.

due to Hg sorption, amalgamation and diffusion processes. Therefore by defining a zero thickness Au sensitive layer, it is proposed that the Au surface maintains its adsorption properties with no bulk related characteristics. Consequently a $\Delta f$ value at zero thickness ($\Delta f_{ads} = \Delta f_{T=0}$) only refers to adsorption and neglects the contributions from Hg amalgamation or diffusion processes, since a zero thickness layer represents only the surface of the film.

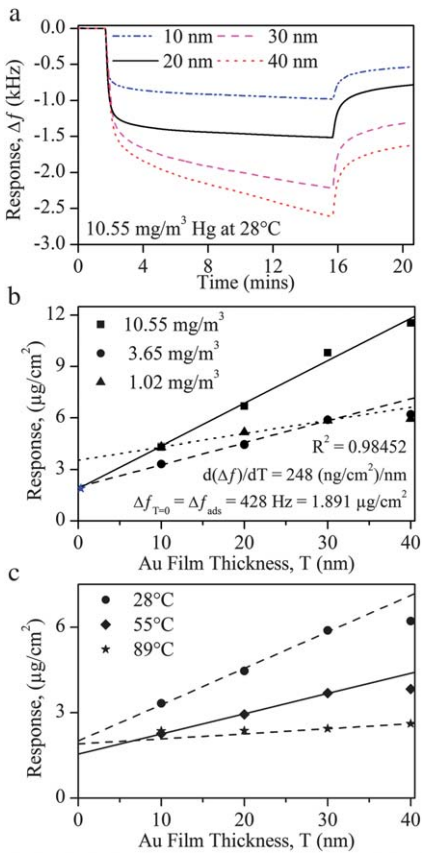


**Fig. 3** (a) Dynamic response of QCM sensors with electrode film thicknesses of 10, 20, 30, and 40 nm when exposed to 10.55 mg $m^{-3}$ Hg at 28 °C, (b) ETZT plots of QCM sensor response when exposed to Hg vapor concentrations of 1.02, 3.65 and 10.55 mg $m^{-3}$ at 28 °C and (c) ETZT plots of QCM sensor response when exposed to Hg vapor concentrations of 3.65 mg $m^{-3}$ at 28, 55 and 89 °C.

Fig. 3a shows the ultra-thin Au sensitive layer based QCMs' response behaviour towards Hg vapor concentration of 10.55 mg $m^{-3}$ at an operating temperature of 28 °C. The sensor response data have been converted from Hz to μg $cm^{-2}$ by using the sensitivity value of 226.4 Hz $cm^2$ $\mu g^{-1}$ using Sauerbrey's equation.[28,29] It may be observed that the 10 and 20 nm Au sensitive layer QCMs reach saturation within the 14 hour Hg exposure period. However the 30 and 40 nm QCMs have a trend of continual Hg uptake throughout the 14-hour exposure time, thus do not reach saturation like the 10 and 20 nm devices. This is primarily attributed to Hg diffusion in the ultra-thin Au sensitive layer. That is, Hg is well known to nucleate and diffuse at surface defects[19] (*i.e.* grain boundaries and kinks), thus releasing the adsorption sites and therefore promoting further Hg sorption to occur at the surface of the film.[15,17,19,30] Fig. 3a shows that the thicker the Au film, the more Hg diffusion occurs and hence an increase in the QCM response magnitude relative to QCMs with thinner Au sensitive layers. As the Hg diffuses into the gold substrate, more Hg is adsorbed on the surface, hence the observed continual drift in response magnitude with time is observed.

Although the 30 and 40 nm QCMs did not reach saturation after 14 hours of Hg vapor exposure at 10.55 mg $m^{-3}$ and an operating temperature of 28 °C, the linear relationship in the ETZT method observed in Fig. 3b is encouraging due to its resemblance to the predicted relationship shown in Fig. 2. Using the ETZT method, it is estimated that the extrapolated *y*-intercept of 428 Hz ($\Delta f_{T=0}$) or 1.891 μg $cm^{-2}$ is due to Hg vapor adsorbing on each of the Au films at the conclusion of the 14 hours of Hg exposure. The slow downward drift or increase in the response signal following the first 5 h (time >6 h on the *X*-axis of Fig. 3a) of Hg exposure period is attributed to slow Hg migration in the bulk of the ultra-thin films of Au, which results in the release of the Hg sorption sites on the Au surface, promoting more Hg vapor to adsorb and amalgamate, as well as migrate into the bulk of the film.

The results in Fig. 3b indicate that the thinner the gold film the higher the observed ratio of the adsorbed to absorbed Hg. For example the 10 nm, 20, 30 and 40 nm Au films were found to contain 43.8, 28.3, 19.3 and 16.4% adsorbed Hg content, respectively, with the balance attributed to absorption/amalgamation, when exposed for a period of 14 hours to Hg vapor concentration of 10.55 mg $m^{-3}$ and an operating temperature of 28 °C. The increase in response magnitude per nanometer of the deposited Au film towards 10.55 mg $m^{-3}$ Hg vapor concentration at 28 °C is estimated by observation based upon the slope/gradient ($d(\Delta f)/\Delta T$) of the extrapolated curve in Fig. 3b at a value of 56.12 Hz $nm^{-1}$ which equates to 248 (ng $cm^{-2}$) $nm^{-1}$. This value is an indication of the relationship between increased film thickness and Hg sorption capacity characteristics of the given Au ultra-thin film. The effect of operating temperature and Hg vapor concentration on the $d(\Delta f)/\Delta T$ and $\Delta f_{T=0}$ values are presented in Fig. 3c.

The ($d(\Delta f)/\Delta T$) value is observed to reduce with either a decrease in Hg exposure concentration or the operating temperature. However, the $\Delta f_{T=0}$ value is observed to decrease with an increase in Hg exposure concentration, but it increases with increasing operating temperature. This indicates that a higher operating temperature increases the ratio of adsorbed to

absorbed Hg on each ultra-thin Au sensitive layer. For example, using the ETZT method, the ratio of amalgamated to adsorbed Hg for the 40 nm Au film ($\Delta f_{T=40}/\Delta f_{T=0}$) following 14 hours of 3.65 mg $m^{-3}$ Hg exposure was estimated to be 2.84 and 1.38 at 55 °C and 89 °C, respectively. The slopes of the ETZT curves were also calculated and found to be only 4 Hz $nm^{-1}$ at 89 °C compared to 16 Hz $nm^{-1}$ at 55 °C. This indicates that Hg sorption has reduced within the film depth at a higher operating temperature. The lower Hg sorption at the higher operating temperature is potentially due to the relatively higher vapor pressure of Hg and therefore its tendency to stay in the vapor phase[31] rather than to adsorb on the Au surface. The surface coverage of Hg would therefore be reduced at the higher operating temperature, thus reducing the flux of Hg through the Au film resulting in less diffused or amalgamated Hg within the bulk of the film during the Hg exposure period.

Following the 14-hour exposure period shown in Fig. 3b, the total response magnitude from the 40 nm thick Au electrode QCM was observed to be 2613.5 Hz at 28 °C and a Hg vapor concentration of 10.55 mg $m^{-3}$. However, as observed in Fig. 3a, most of the sorption occurred in the first 300 minutes of Hg exposure time (between 100 and 400 min on the *X*-axis of Fig. 3a) at which stage the sensor response was recorded to be 2078.8 Hz. This potentially means that ~535 Hz or 2362 ng $cm^{-2}$ of Hg had diffused in the subsequent 540 minutes of Hg exposure resulting in the average diffusion rate of ~72.9 pg $cm^{-2}$ $s^{-1}$. Similarly the calculated diffusion rate for the 10, 20 and 30 nm ultra-thin Au sensitive layers was found to be 10.4, 11.9 and 47.9 pg $cm^{-2}$ $s^{-1}$, respectively. This indicates that the thicker the Au film, the higher the Hg diffusion rate or uptake. In order to remove the diffusion contribution, a line of best fit representing diffusion was subtracted from the QCM response during the Hg exposure period, an example of which is shown in Fig. 4a for the 40 nm

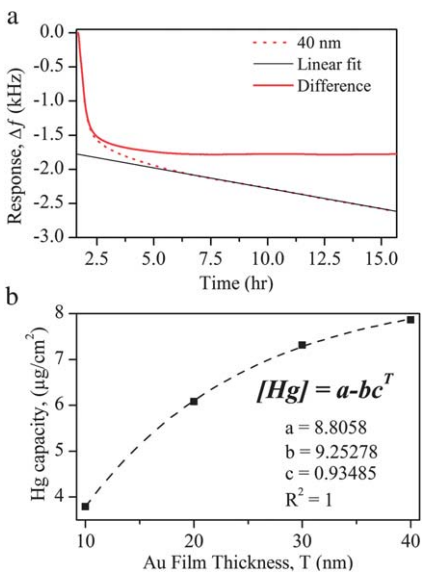


**Fig. 4** (a) QCM dynamic response, showing the fitted diffusion contribution (linear fit) in dynamic response for a 40 nm ultra-thin Au sensitive layer and (b) response magnitudes of QCM sensors with ultra-thin Au sensitive layer thicknesses of 40 nm after removing the diffusion contribution when exposed to 10.55 mg $m^{-3}$ Hg for 14 hours at 28 °C.

QCM exposed to Hg vapor at 28 °C and Hg concentration of 10.55 mg $m^{-3}$ for 14 hours. The response magnitude of the modified response was then plotted with Au film thickness as shown in Fig. 4b.

It is observed that the Hg capacity (that is without the diffusion contribution) increases with Au film thickness and fits well ($R^2 = 1$) with the asymptotic equation of $[Hg] = a - bc^T$ as shown in Fig. 2b. The parameters *a*, *b* and *c* are constants while *T* represents the Au film thickness (nm) and [Hg] represents the Hg concentration in the Au film (μg $cm^{-2}$). From the equation it was calculated that by using a 40 nm Au sensitive layer 92.6% of the limit was reached at 7.88 μg $cm^{-2}$ of Hg coverage on Au ultra-thin film deposited on $SiO_2$. From the asymptotic equation, a 70 nm film reaches close to the 100% limit (8.806 μg $cm^{-2}$). That is, any additional Hg would only diffuse through the 70 nm Au film. Since the amount of Hg diffused follows a linear relationship with the exposure time under set conditions (*i.e.* operating temperature and Hg vapor concentration in the vapor phase), it follows that all this Hg may be diffusing right down the bottom of the Au layer and accumulating. In order to determine the diffusion behaviour of Hg through the Au films, SIMS depth profile was performed on the samples and the results are presented in the next section. With the adsorbed Hg (428 Hz) on any of the Au surfaces under these conditions equates to 1891 ng $cm^{-2}$. Since one nominal monolayer of Hg on gold is equivalent to 469 ng $cm^{-2}$ (ref. 30) and using the electrochemical surface area (1.5 $cm^2$ $cm^{-2}$) of Au films calculated in previous work,[5] this value may be converted to 2.69 nominal monolayers of Hg (or 4 monolayers if the mechanical surface area of 0.32 $cm^2$ was used).[15] These values are in line with the literature[17,32,33] where Hg has been reported to not make a full monolayer on the Au surface and that several nominal Hg monolayers are required before amalgamation may take place. Under the Hg exposure conditions used in this work, it may be that amalgamation initiates following ~2.69 nominal monolayers of adsorbed Hg where the ratio of Hg atoms to Au atoms is satisfied.[34] One method to confirm amalgamation of Au with Hg is by observing the morphology change of the Au surface which occurs following the exposure of Au to elemental Hg vapor. The SEM images of the QCM sensors with electrode film thicknesses of 10, 20, 30, and 40 nm before and after exposure to Hg vapor concentration of 10.55 mg $m^{-3}$ for 14 h followed by 5 h of recovery period at an operating temperature of 28 °C are shown in Fig. S1 (see ESI†). It is observed that the surface morphology of each electrode has undergone a change following Hg exposure, as in agreement with previous studies.[35]

### Hg diffusion in ultra-thin Au sensitive layers

To determine the characteristics of how Hg diffuses and migrates into the bulk of Au thin films, SIMS depth profiling was performed on selected samples. The SIMS depth profiles for a clean 40 nm Au control QCM (which was not exposed to Hg vapor) and a 40 nm Au QCM which was exposed to Hg at 10.55 mg $m^{-3}$ for a period of 14 hours followed by 5 hours of recovery period, at an operating temperature of 28 °C, are shown in Fig. 5.

The SIMS counts for each element have been normalised with the primary $Cs^+$ ion counts (*Y*-axis). The *X*-axis represents the sputter time (in seconds) and ultra-thin Au sensitive layers' depth

 

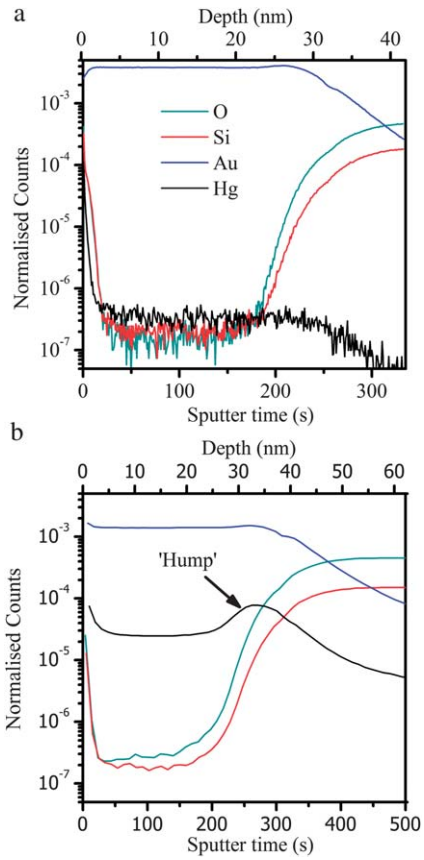


**Fig. 5** SIMS depth profile of the ultra-thin Au sensitive layers exposed to 10.55 mg $m^{-3}$ Hg at an operating temperature of 28 °C.

(in nm) where depth profilometer measurements from one of the Au ultra-thin samples (20 nm) showed ~328 seconds of etching time equates to 40.7 nm of etching depth. Since the etching rate from the beam line was partially different from day to day, both sputter time and the conversion of it to the Au film depth have been plotted on the *X*-axis. This method is used for all subsequent SIMS depth profiles presented in this manuscript.

As expected, Fig. 5a shows no Hg is present throughout the Au depth in the 40 nm thick control sample where no Hg has been exposed. Furthermore, the Au counts are observed to decrease with sputter time while the Si and O counts increase substantially after 200 seconds of etching, thus confirming the existence of the $SiO_2$ barrier film beneath the ultra-thin Au sensitive layer. Fig. 5b shows that when the same 40 nm Au film is exposed to Hg vapor, a small amount of Hg is present on the surface which quickly decreases with increasing depth of the Au layer (<20 seconds). However as the Au signal reduces with the Au film depth at the point where Si and O signals are observed to increase, the Hg signal is observed to increase (shown by the 'Hump' marking) and thereafter reduce with the Au profile to noise level once maximum Si and O signals are reached. The presence of the 'hump' at 250 seconds is indicative that the Hg vapor migrates throughout the depth of the Au layer until it reaches the $Au/SiO_2$ interface. Similar humps were also observed for the 20 and 30 nm Au sensitive layers, however no such obvious hump is observed for the 10 nm ultra-thin Au sensitive layer, as shown in Fig. 6.

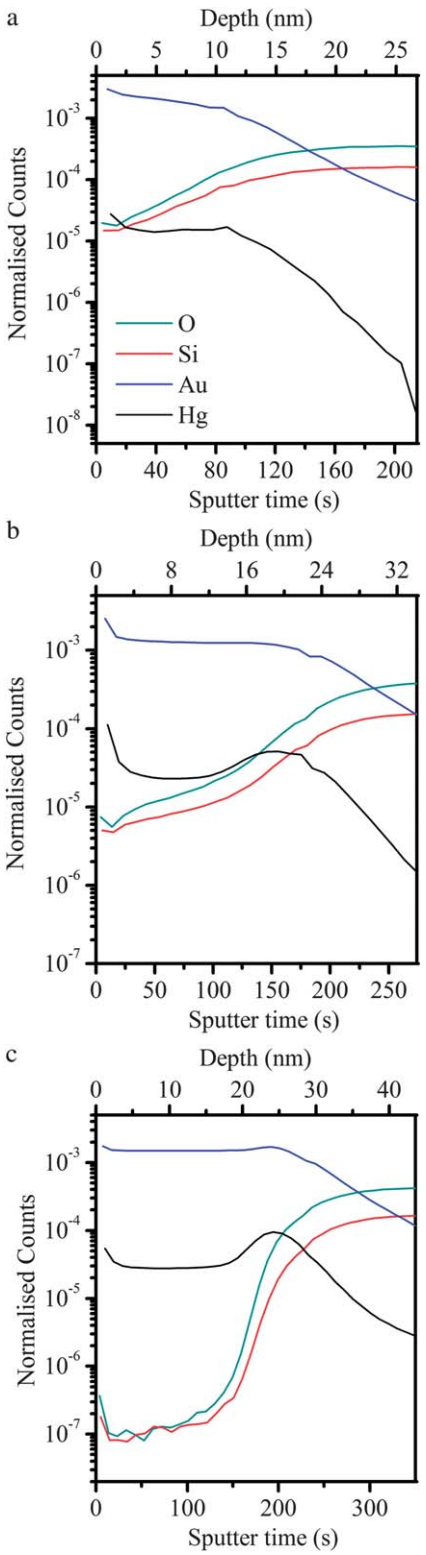


**Fig. 6** SIMS depth profiles of the ultra-thin Au sensitive layers exposed to 10.55 mg $m^{-3}$ Hg at an operating temperature of 28 °C.

The humps on the 20, 30 and 40 nm samples show that Hg does not diffuse through the $SiO_2$ layer, and thus is unable to migrate from the ultra-thin Au sensitive layers down into the underlying 150 nm Au electrodes of the QCMs.

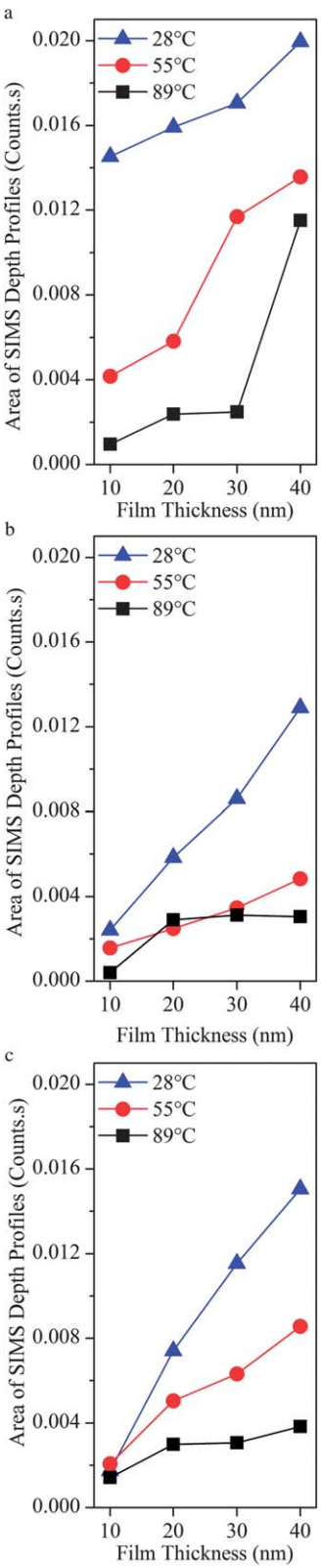


**Fig. 7** The area under the SIMS depth profiles (in counts per second) showing the influence of operating temperature and Hg vapor concentration on the amount of diffused and accumulated Hg in the ultra-thin Au sensitive layers.

More importantly, the increase in the Hg counts at the interface (humps) shows the accumulation of Hg at the Au/$SiO_2$ interface as was presumed. Be'er *et al.*[18] have also observed similar behaviour of elemental Hg droplets, which spread and diffuse through gold and accumulate at the Au/$SiO_2$ interface. The decrease in Hg counts following the hump is observed to be similar to the trend for gold indicating that the $SiO_2$ layer may have contained some pores containing Au which amalgamated with Hg. The normalised Hg counts for each Au thickness are summarised in Fig. S2 (see ESI†). The position of the humps maxima on the *X*-axis is observed to correspond to the thickness of the ultra-thin Au sensitive layers used in the analysis. It should be noted that the area under the curve is directly proportional to the amount of Hg available in the region. It can be clearly observed that the area under the humps appears to be larger as the Au thickness increases. This is attributed to more amalgamated Hg with the thicker Au electrodes, as may be observed from the QCM response curves in Fig. 3a.

Since Hg diffusion is dependent on the amount of Hg present at the Au surface,[15] and in turn is influenced by the operating conditions, some differences in diffusion behaviour are observed on each ultra-thin Au sensitive layer under each of the tested operating conditions. The data presented in Fig. 7 show a summary of the integration of the SIMS depth profiles (hump areas) of each of the ultra-thin Au sensitive layer exposed to Hg vapor under different operating conditions.

Due to the lack of SIMS Au–Hg standards, it was not possible to qualitatively deduce the concentration of Hg, and as such the data presented only refer to the relative amount of Hg present in each case. The results presented in Fig. 7 confirm that the relative amount of accumulated Hg increases with increasing Au film thickness as well as decreasing operating temperature. This is attributed to the increased Hg sorption which occurs when the operating temperature is decreased.

## Conclusions

In an attempt to differentiate between Hg adsorbed and Hg absorbed on ultra-thin Au sensitive layers, the response magnitude of each set of sensors was used to extrapolation to zero thickness (ETZT) for the 9 different operating conditions. In general, the ratio of adsorbed to absorbed Hg on Au films is found to decrease with increased Hg vapor concentration. This ratio was also found to increase with increased operating temperature. QCM data showed that there was a significant amount of mercury accumulating in the ultra-thin Au sensitive layers. In order to show this experimentally, SIMS depth profiling of all QCMs was performed and confirmed that Hg penetrates and diffuses through Au thick films. Furthermore, it was found that following diffusion processes, Hg accumulation occurs between the ultra-thin Au sensitive layer and the $SiO_2$ barrier layer. It was found that significant Hg accumulation occurred in the 20, 30 and 40 nm layers but not to the same extent in the 10 nm ultra-thin Au sensitive layers. This indicated that in order to reduce Hg accumulation in Au, a non-continuous type film (similar to the 10 nm ultra-thin Au sensitive layers morphology) would hold more positive characteristics when utilised as a Hg sensitive layer. The Hg sensor would perform well, given the film could be fabricated directly onto QCM

electrodes with a high surface to volume ratio which could ensure a large response magnitude. On the other hand, a continuous type thick Au film is also believed to perform well however there would be a significant amount of Hg accumulation in the sensitive film which could potentially reduce the lifetime of the sensors.

## Acknowledgements

We would like to acknowledge the Australian Research Council (ARC) for supporting this project (grant number LP100200859, the RMIT microscopy and microanalysis facility (RMMF) for allowing the use of their comprehensive facilities and services. SI acknowledges ARC for APDI fellowship. The authors would like to acknowledge the support from the Australian Institute of Nuclear Science and Engineering (AINSE) for providing access to SIMS under an AINSE grant: ALNGRA11137.

## Notes and references

1 C. Senior, C. J. Montgomery and A. Sarofim, *Ind. Eng. Chem. Res.*, 2010, **49**, 1436–1443.
2 E. B. Swain, P. M. Jakus, G. Rice, F. Lupi, P. A. Maxson, J. M. Pacyna, A. Penn, S. J. Spiegel and M. M. Veiga, *Ambio*, 2007, **36**, 45–61.
3 G. V. Ramesh and T. P. Radhakrishnan, *ACS Appl. Mater. Interfaces*, 2011, **3**, 988–994.
4 Y. M. Sabri, R. Kojima, S. J. Ippolito, W. Wlodarski, K. Kalantar-zadeh, R. B. Kaner and S. K. Bhargava, *Sens. Actuators, B*, 2011, **160**, 616–622.
5 Y. M. Sabri, S. J. Ippolito, A. P. O'Mullane, J. Tardio, V. Bansal and S. Bhargava, *Nanotechnology*, 2011, **22**, 305501.
6 T. P. McNicholas, K. Zhao, C. Yang, S. C. Hernandez, A. Mulchandani, N. V. Myung and M. A. Deshusses, *J. Phys. Chem. C*, 2011, **115**, 13927–13931.
7 P. Selid, H. Xu, E. M. Collins, M. Striped Face-Collins and J. X. Zhao, *Sensors*, 2009, **9**, 5446–5459.
8 T. Morris, K. Kloepper, S. Wilson and G. Szulczewski, *J. Colloid Interface Sci.*, 2002, **254**, 49–55.
9 E. P. Scheide and J. K. Taylor, *Environ. Sci. Technol.*, 1974, **8**, 1097–1099.
10 Y. M. Sabri, S. J. Ippolito, A. J. Atanacio, V. Bansal and S. K. Bhargava, *J. Mater. Chem.*, 2012, DOI: 10.1039/c1032jm33480a.
11 A. Janshoff, H.-J. Galla and C. Steinem, *Angew. Chem., Int. Ed.*, 2000, **39**, 4004–4032.
12 J. Li and H. D. Abruna, *J. Phys. Chem. B*, 1997, **101**, 2907–2916.
13 P. D. Sawant, Y. M. Sabri, S. J. Ippolito, V. Bansal and S. K. Bhargava, *Phys. Chem. Chem. Phys.*, 2009, **11**, 2374–2378.
14 V. Raffa, B. Mazzolai, V. Mattoli, A. Mondini and P. Dario, *Sens. Actuators, B*, 2006, **114**, 513–521.
15 Y. M. Sabri, S. J. Ippolito, J. Tardio, A. J. Atanacio, D. K. Sood and S. K. Bhargava, *Sens. Actuators, B*, 2009, **137**, 246–252.
16 C. Battistoni, E. Bemporad, A. Galdikas, S. Kaciulis, G. Mattogno, S. Mickevicius and V. Olevano, *Appl. Surf. Sci.*, 1996, **103**, 107–111.
17 M. Levlin, E. Ikavalko and T. Laitinen, *Fresenius' J. Anal. Chem.*, 1999, **365**, 577–586.
18 A. Be'er, Y. Lereah, A. Frydman and H. Taitelbaum, *Phys. A*, 2002, **314**, 325–330.
19 M. A. George and W. S. Glaunsinger, *Thin Solid Films*, 1994, **245**, 215–224.
20 Y. M. Sabri, S. J. Ippolito, J. Tardio and S. K. Bhargava, *J. Phys. Chem. C*, 2012, **116**, 2483–2492.
21 J. Crank, *The Mathematics of Diffusion*, Oxford University Press, London, England, 1975.
22 P. W. Atkins, *Physical Chemistry*, Oxford University Press, Oxford, Great Britain, 1982.
23 H. K. Chaurasia, A. Huizinga and W. A. G. Voss, *J. Phys. D: Appl. Phys.*, 1975, **8**, 214–218.
24 J. J. McNerney, P. R. Buseck and R. C. Hanson, *Science*, 1972, **178**, 611–612.
25 G. C. T. Wei and B. J. Wuensch, *J. Am. Ceram. Soc.*, 1976, **59**, 295–299.
26 R. L. B. Haskell, J. J. Caron, M. A. Duptisea, J. J. Ouellette and J. F. Vetelino, in *Ultrasonics Symposium, 1999. Proceedings, IEEE*, Orono, ME, 1999, vol. 421, pp. 429–434.
27 Y. M. Sabri, in Applied Sciences, PhD thesis, RMIT University, Melbourne, 2010, p. 271.
28 G. Sauerbrey, *Z. Phys. A: Hadrons Nucl.*, 1959, **155**, 206–222.
29 B. Zimmermann, R. Lucklum, P. Hauptmann, J. Rabe and S. Büttgenbach, *Sens. Actuators, B*, 2001, **76**, 47–57.
30 T. Morris, J. Sun and G. Szulczewski, *Anal. Chim. Acta*, 2003, **496**, 279–287.
31 I. Sanemasa, *Bull. Chem. Soc. Jpn.*, 1975, **48**, 1795–1798.
32 H. J. F. Jansen, A. J. Freeman, M. Weinert and E. Wimmer, *Phys. Rev. B*, 1983, **28**, 593.
33 A. R. Miedema and J. W. F. Dorleijn, *Philos. Mag. B*, 1981, **43**, 251–272.
34 X. Yang, K. Tonami, L. A. Nagahara, K. Hashimoto, Y. Wei and A. Fujishima, *Chem. Lett.*, 1994, **11**, 2059–2062.
35 M. Fialkowski, P. Grzeszczak, R. Nowakowski and R. Holyst, *J. Phys. Chem. B*, 2004, **108**, 5026–5030.